Journal of Physics: Conference Series

SIMS and RBS Investigation of Zn Implanted Si

To cite this article: V S Kulikauskas *et al* 2011 *J. Phys.: Conf. Ser.* **281** 012031

Journal of Physics: Conference Series **281** (2011) 012031 doi:10.1088/1742-6596/281/1/012031

SIMS and RBS Investigation of Zn Implanted Si

V S Kulikauskas[1], V V Saraykin[2] and V V Privezentsev[3]

[1]Skobel'tsyn Institute of Nuclear Physics, Lomonosov Moscow State University, Leninskie Gory, 119991 Moscow, Russia
[2] Research Institute of Physical Problems, Zelenograd, 124460 Moscow, Russia
[3]Institute of Physics & Technology, Russian Academy of Sciences, Moscow 117218, Russia

E-mail: privezentsev@ftian.ru

Abstract. We present results of secondary ion mass-spectrometry and Rutherford backscattering spectroscopy of the Zn implantation profile in the damaged layer of a n-type Cz-Si(100) substrate, as well as the profile change during annealing. Si wafers were implanted with $^{64}Zn^{+}$ ions at energy of 100keV and ion dose of $2\times10^{14}cm^{-2}$. They were then subsequently annealed at 400°C for 60min and 700°C for 10min. Analysis of experimental data shows that in the as-implanted sample on a silicon surface a damage gauzy amorphous layer with thickness about 80nm was created, located inside the substrate at the ion-implantation depth. After two annealing steps the defects were completely annealed out. From the Zn depth profiles we observe that during annealing the Zn concentration decreases and the Zn peak concentration moves to the wafer surface. The Zn concentration maximum exceeds the solubility limit of Zn in Si, suggesting decomposition of Zn solid solution in Si and Zn precipitation.

1. Introduction

The properties of metal and metal oxide nanoparticles (NPs) in various matrices have been the subject of recent study since such nanostructured materials can be used in modern electronic devices [1]. Among them metallic Zn NPs play an important role. These NPs in a Si substrate can be made in particular by Zn ion implantation with subsequent processing of a Si wafer by various ways. Recrystallization of the damage Si layers implanted by Zn can be induced either thermally [2, 3], by pulsed laser irradiation [4], or by means of an ion beam [5].

Zn implantation of Si with subsequent annealing in neutral (inert) and oxygen atmosphere is the key fabrication stage during Zn NP formation, which subsequently transforms to ZnO NPs. Therefore study of the microstructural properties of such material becomes highly relevant. Ion implantation of metallic elements in semiconductors may result in the precipitation of metallic NPs in the implanted layer. It can occur either during the implantation [6] or the subsequent annealing stage [7]. Regarding high-dose Zn implantation in Si, it has been demonstrated that nanoscale hexagonal Zn and ZnO inclusions can be precipitated directly during implantation at room temperature [8].

For elements like Zn with combined diffusion mechanisms (interstitial/substitutional), the depth concentration profiles after annealing will be influenced by implantation induced defects. The ion implantation process will generate a high defect density in the Si crystal substrate and can amorphize it at doses above $10^{15}cm^{-3}$. The interaction of these defects and diffusing implanted atoms and also the recrystallization of the amorphous Si layer will have a strong influence on the diffusion of the implanted elements during annealing steps. Beside this the precipitation of the supersaturated solid solutions and intermediate compounds may occur at structural defects [4, 5].

Therefore a study of the properties of such material becomes highly relevant. Here we present a Rutherford back scattering (RBS) investigation of damaged layer and secondary ion mass-spectrometry (SIMS) investigation of Zn implanted profile in Si substrate, and examine how these profiles change during annealing.

2. Experimental Technique

A single crystal wafer of n-type Cz-Si(001) with thickness of 350μm and electron concentration of 3×10^{15}cm^{-3} was implanted with $^{64}Zn^{+}$ ions at an energy of 100keV and ion dose 2×10^{14}cm^{-2}. The ion beam current density of 60nA/cm^2 and a 2mm diameter was scanned over the substrate surface at an angle of 7^o. The samples were subsequently annealed in a nitrogen atmosphere at 400°C for 60min and in an argon atmosphere at 700°C for 10min. Irradiation defects in a test sample were investigated by RBS of 2MeV He ions using ion channelling.

Secondary ion mass spectrometry (SIMS) was performed using a CAMECA IMS-4f at 150nA. Primary O_2^+ions with energy 10keV were used and mass-spectral resolution was 4000. The focused primary beam was rastered over an area of 200×200μm^2, with detection of ions from a circular area of 60μm diameter at the raster centre. The sputtering rate was approximately 0.5nm/s.

3. Results

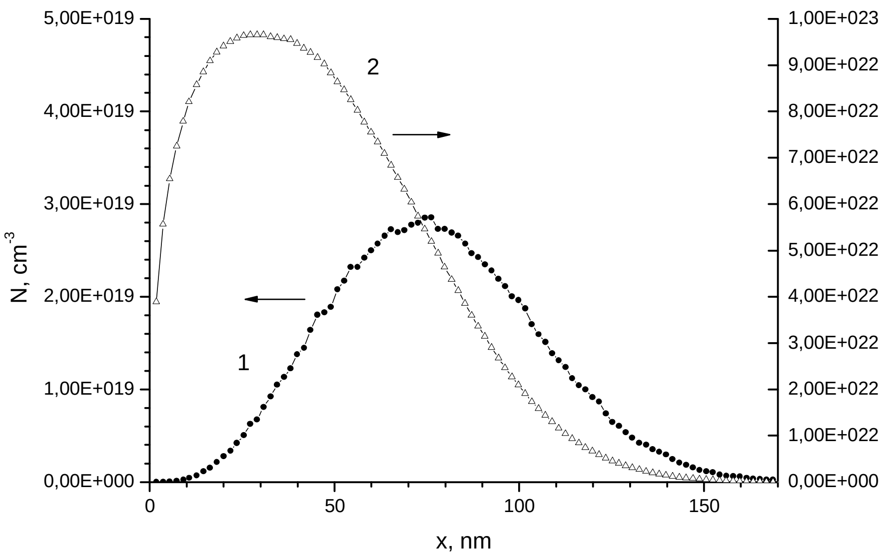

Figure 1. SRIM soft simulation results of distribution of implanted s $^{64}Zn^{+}$ ion (1) and Si target displaced atoms (Frenkel pair) (2)

According to SRIM simulation [10] the projected length for Zn ions is about 76nm for the given implantation conditions (figure 1, line 1). The $^{64}Zn^{+}$ ion produces about 2300 displacements of Si matrix atoms (radiation induced Frenkel pairs). Its distribution maximum is located at a depth of about 30nm (figure 1, line 2).

The experimental and simulated random and experimental aligned RBS spectra of He^+ ions for test samples are presented in figure 2. On the right side of the aligned RBS spectra there is a peak. As for the implanted sample the value of this peak in the aligned spectrum does not match that of a random spectrum, so the damaged layer is not completely amorphous. During annealing the value of this peak and its width decrease. If we assume that the damaged layer is completely amorphous, then it is possible to define a superficial density of the interstitial atoms of a Si matrix and this layer thickness [11]. It has been as a result found that after implantation the damaged layer thickness is 78nm, and the surface density of the interstitial atoms of a Si matrix is $3.9\times10^{17}cm^{-2}$. After preliminary annealing at 400^oC for 60 minutes in a nitrogen atmosphere the damaged layer thickness decreases to 56nm and the surface density of the interstitial atoms decreases to $2.8\times10^{17}cm^{-2}$. After the final high-temperature anneal at 700^oC for 10minutes in an argon atmosphere the damaged layer almost completely disappears and its thickness is only 2.0nm. Thus the associated density of interstitial atoms in the Si matrix is $1.0\times10^{16}cm^{-2}$. The aligned spectrum also shows peaks due to the presence of oxygen and carbon in the test sample. Their associated surface density is $N_O=4.4\times10^{17}cm^{-2}$ and $N_C=1.2\times10^{17}cm^{-2}$.

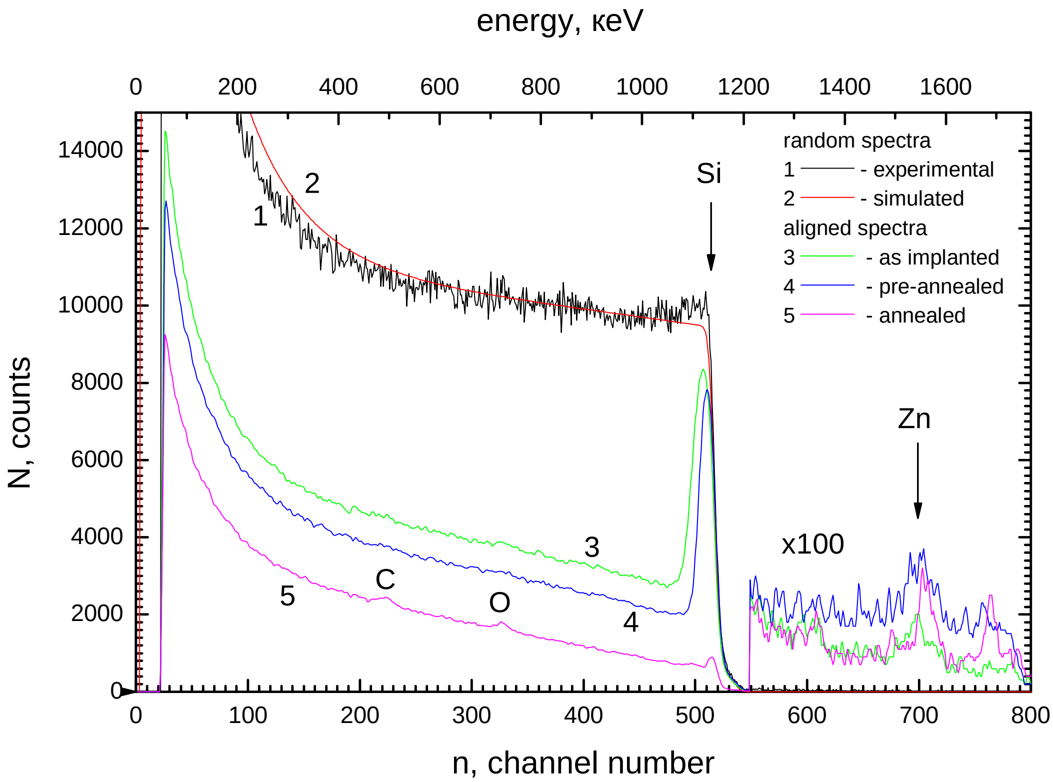

Figure 2. RBS patterns from Si wafers implanted with $^{64}Zn^+$ ions, random spectra (1) – experimental, (2) – simulated (on Fig.2, right they are not shown); aligned spectra: (3) – as implanted, (4) – pre-annealed at 400^oC, (5) – annealed at 400^oC + 700^oC. Vertical arrows note channels of the particle scattering on the sample surface by ^{28}Si and ^{64}Zn atoms

Figure 3 shows the SIMS Zn depth profiles for the investigated samples. For the as-implanted sample the Zn distribution in depth profile (line 1) has a maximum at a depth of 75nm. line 2 shows SIMS spectrum of the implanted sample with pre-annealing at 400^0C in nitrogen atmosphere for 60min. This also shows segregation to the right side of the concentration maximum. Particularly, we note that the value of displacement maximum has not changed, but its intensity has increased. Line 3 in figure 2 presents the sample annealed at 400^oC in nitrogen atmosphere + 700^oC in argon atmosphere. This curve shows two concentration peaks. The first curve maximum lies near the sample surface at depth less than 20nm. This peak is strong and consists of more than $5\times10^{19}cm^{-3}$. The second one occurs at a depth of 40nm near the projected range for the Zn ion implantation. Its intensity is higher than the limiting equilibrium concentration of Zn in Si.

4. Discussion.

In the as-implanted sample a damage layer with thickness about 78nm was formed near the sample surface. The radiation-induced point defects (Frenkel pairs) make the major contribution to the damage due to large amount of displacements per implanted Zn ion (about 2300). We note that as in the implanted sample, the radiation damage of the Si lattice and defect formation are determined by redistribution of radiation-induced point defects owing to secondary processes: annihilation of intrinsic interstitial Si atoms and vacancies, and a sink of interstitial Si atoms at the sample surface. One maximum is visible on the profile of Zn distribution in the depth profile for the as-implanted sample (figure 3, line 1). In this layer the Zn concentrations are considerably above the equilibrium limit of Zn solubility in Si namely $N_{Zn}^{lim}=6\times10^{16}cm^{-3}$ [13].

After pre-annealing at 400°C the damage layer thickness decreases to about 56nm. Because of high mobility of interstitial Si atoms and due to their sink towards a substrate surface the subsurface area is enriched by defects of vacancy type. Probably, these defects are clusters of intrinsic Si vacancies and/or complexes Si vacancy – Zn atom. Annealing leads to thermal activation of secondary processes and enrichment of a sample surface by vacancy type defects. This effect is observed as a reduction of the aligned RBS spectrum in a subsurface area.

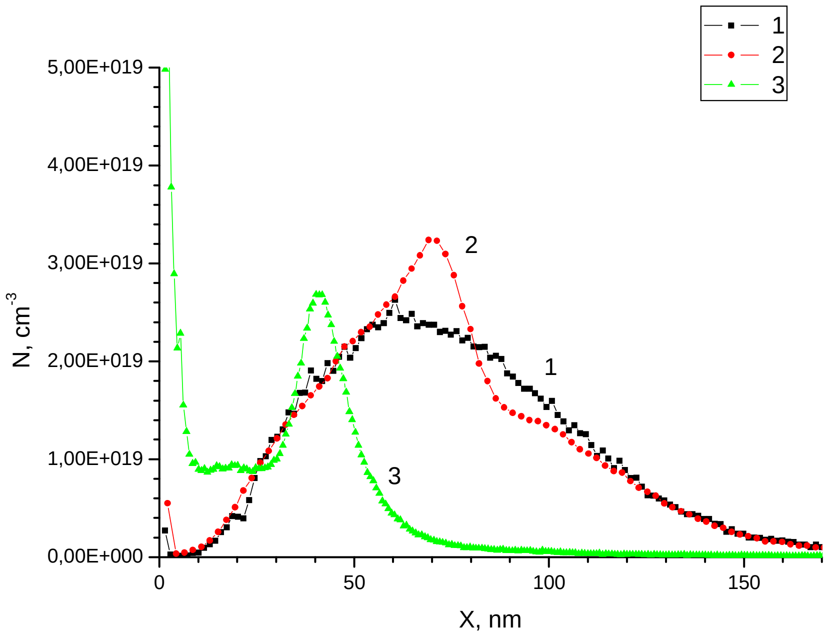

Figure 3. SIMS Zn distribution profiles on the depth, samples: as-implanted (1), pre-annealed at 400°C (2) and annealed at 400°C+700°C (3)

It is known that diffusion of Zn in Si proceeds by a mixed mechanism (interstitial/substitution) [13]. After pre-annealing at 400°C the feature in Zn concentration distribution at nearby 70nm can be caused by Zn diffusion towards the sample surface and into substrate depth, which interfere in two defect areas. One of them is enriched in intrinsic radiation-induced interstitial defects and is displaced at a depth nearby 30nm. Here, according to SRIM, there is a maximum of the displaced atoms (Frenkel pairs) distribution. Generated Frenkel pairs create damage in a crystal lattice, and the associated depth distribution is presented in figure 1, line 2. The second area is displaced to nearly 100nm, and has enriched so-called “end-of-range” defects. These defects are in a tail of impurity atom distribution behind its maximum, representing the small clusters of intrinsic radiation-induced interstitial defects, which are not yet annealed at 400°C.

After annealing at 700°C a reduction of point defect density and the complexes responsible for damage of the matrix crystal lattice is observed (figure 2, spectrum 5). The damage layer thickness has decreased to 2.0nm, and the density of the Si matrix interstitial atoms to $1.0\times10^{16}cm^{-2}$. Radiation-induced defects in the sample have almost all annealed out. Reconstruction of the radiation-induced damage layer has occurred from the intrinsic substrate and, apparently, most defects have diffused deep into the substrate. On the other hand the subsurface area has become enriched with Si vacancies due to the sink of interstitial Si atoms towards the crystal surface. In the damage layer near the interface with the intrinsic substrate there are located the weakly associated intrinsic interstitial Si atoms. RBS spectra for all studied sample temperature treatments demonstrate the same behavior (decrease of intensity and width) of the peak in figure 2 (spectra 4 and 5). Thus, the damaged layer thickness and interstitial Si atom density decrease during annealing in all samples. It means that the radiation-induced point defects in the damaged layer are relaxed through interaction with participating Si matrix interstitials and Zn impurity atoms, due to them clustering.

After annealing at 700^{o}C there is an active redistribution of impurity Zn in the area of the damaged layer, therefore a Zn distribution in the depth profile (figure 3, curve 3) has undergone significant changes. Now in the SIMS spectra there are two concentration peaks: one located at the sample surface and another in the substrate depth. The first area thickness is less than 10nm, at the subsurface Zn concentration peak. On the substrate surface this depth is associated with a silicon oxide layer, which is an effective sink for Zn atoms. So this peak is connected with a Zn atom sink near the sample surface. The maximum near the sample surface corresponds to distortions of the crystal lattice, which are caused by association of radiation-induced point defects, which sink towards the crystal surface.

The second area is located in the subsurface region where the majority of Zn atoms are gathered. In this area another Zn concentration peak is located at depth of 40nm. After the second annealing the peak grows and moves closer to a sample surface (figure 3, comparing curves 2 and 3). This shows Zn atom clustering during precipitation from the super saturation solid solution of Zn in Si. High temperature annealing results in further growth of the Zn clusters. This peak is thus apparently caused by radiation-induced defects, which have formed clusters near the sample surface, which interfere with the fast Zn atom diffusion to the sample surface. The second peak corresponds to a depth where, according to SRIM simulations, the number of Si matrix atom displacements due to irradiation is a maximum. This peak occurs at a depth before the projected range, which is the most probable penetration depth for the implantation. For example, the projected range for Zn ion implantation is 75nm [10] and the second peak occurs at 40nm. Thus such obstacles do not exist at greater depths. A similar situation was observed in [4], where implantation and annealing were occurred under approximately similar conditions. This concentration peak transformation could also be due to the formation of Zn-silicide compounds ($ZnSiO_3$ type).

A third peak sometimes also occurs [4], deeper than the implant projected range. It is related to implantation defects at range end. At sufficiently high dozes this maximum is related to amorphous and damaged parts of the substrate.

During Zn ion implantation in the Si substrate and subsequent thermal annealing stages the initial process is characterized by Zn precipitation and formation of Zn-silicide (type of $ZnSiO_3$) compound due to HRXRD. The oxygen dissolved in Cz-Si can take part in this reaction leading to such formation. From IR-spectroscopy data the oxygen concentration in the initial Si wafer was about $N_O=6\times10^{17}cm^{-3}$.

5. Conclusions

PBS and SIMS spectral distribution in the as-implanted state is determined by redistribution of radiation induced point defects due to secondary processes (annihilation of Si intrinsic interstitial atoms and vacancies, a sink of interstitial defects towards the sample surface). The 78nm subsurface layer is disordered.

Heat treatment at 400^{o}C for 1h leads to annealing of interstitial point defects and a thickness reduction of the damaged Si lattice layer to 56nm. This layer contains clusters or Zn- vacancy complexes. These complexes result from reactions between vacancies and implanted Zn atoms activated by thermal annealing. In the area enriched by Si interstitials the annealing stimulates Zn precipitation from Si<Zn> solid solution.

After annealing at 700^{o}C for 10min the damage layer has reconstructed almost completely. A sharp redistribution of Zn was observed in this sample. The total amount of Zn in the layer decreased, which was probably caused by diffusion deep into the Si substrate. High temperature annealing contributes to further growth of the Zn clusters.

References

[1] Redel E. Transition Metal Nanoparticles. Sudwestdeutscher Verlag Fur Hochschulschrifte, 2009.
[2] Henry M O, Campion J D, McGuigan K G, Wthewalt M L and Lightowlers E C 1989 *Mater. Sci. Eng. B* **4** 201.
[3] Simov S, Kalitzova M, Karpuzov D, Yankov R, Angelov Ch, Faure J, Bonhomme P and Balossier G 1996 *J. Appl. Phys.* **79** 3470.
[4] Francois-Saint-Cyr H, Anoshkina E, Stevie F, Chow L, Richardson K and Zhou D 2001 *J. Vac. Sci. Technol. B* **19** 1769.
[5] Eryu O, Murakami K, Takita K and Masuda K 1988 *Nucl. Instr. Meth. Phys. Res. B* **33** 665.
[6] Lohner T, Angelov C and Mikli V 2008 *Thin Solid Films* **516** 8009.
[7] Kalitzova M, Simov S, Yankov R A, Angelov C, Vitali G, Rossi M, Pizzuto C, Zollo G, Faure J, Killan L, Bonhomme P and Voelskov M 1997 *J. Appl. Phys*. **81** 1143.
[8] Zollo G, Kalitzova M, Manno D and Vitali G 2004 *J. Phys. D: Appl Phys.* **37** 2730.
[9] Muntele I, Thevenard P, Muntele C, Chhay B and Ila D 2005 *Mater. Res. Symp. Proc.* **829**, paper B.2.21.
[10] http://www.srim.com/
[11] http://www.simnra.org/
[12] Feldman L C and. Mayer J W Fundamentals of surface and thin film analysis. North-Holland, NY-Amsterdam-Londom 1986.
[13] Milnes A. Deep Impurities in Semiconductors. Wiley, NY - London 1973.